

PREDICTION OF CONFINED COMPRESSIVE STRENGTH OF SQUARE CONCRETE COLUMNS BY ARTIFICIAL NEURAL NETWORKS

Ertekin Öztekin

Dept. of Civil Engineering, Gumushane University, Baglarbasi 29100 Gumushane, Turkey
E-mail address: ertekinoztekin@gumushane.edu.tr

Abstract

This paper presents the application of artificial neural networks (ANN) for prediction of confined compressive strength of square concrete columns. Experimental data of 252 normal and high strength square concrete column were collected from the literature to develop an ANN model with input parameters consisting of yield strengths, numbers and diameters of longitudinal and transverse reinforcements, characteristic concrete strength, concrete cover thickness, specimen dimension, transverse reinforcement spacing and six different transverse reinforcement configurations. Confined compressive strength predictions of square concrete columns by ANN were compared to some analytical models and were found very promising.

Keywords: Artificial neural network (ANN), confined concrete, confined concrete strength, compressive strength, concrete column.

1. Introduction

The influences of different parameters on confined compressive strength, comparing them to unconfined concrete behavior, have been investigated in both analytical and experimental studies by a lot of researchers. So many analytical models have been developed for prediction of stress-strain relationship and confined compressive strength for concrete column. Some of these models were presented in the literature by Sheikh and Uzumeri [1], Soliman and Yu [2], Sargin [3], Nagashima [4], Yong et al [5], Mugurama [6], Fafitis-Shah [7], Kappos [8], Mander [9]. The proposed analytical models were developed based on a specific set of experimental data. Hence, while these models produced closer predictions to their own experimental results, their predictions could not be close to the results of different experiments. This might be attributed to the differences in the parameters such as transverse reinforcement volumetric ratio, longitudinal reinforcement ratio, concrete strength, transverse reinforcement spacing, concrete cover, yield strengths of longitudinal and transverse reinforcements, specimen dimensions, transverse reinforcement configuration etc. These parameters were defined as variables to investigate their effects on confined concrete behavior in different studies in literature.

Hong et al [10] performed an experimental study to determine low-volumetric-ratio lateral tie effects on high strength concrete. Suzuki et al [11] proposed a stress strain model for high strength concrete confined by rectangular ties. Song et al [12] conducted experiments and analyses to investigate confining effect of confined concrete columns having different core sizes, spacing ratios and transverse reinforcement ratios. Sakai et al [13] tested 18 short tied columns to examine the confinement effects of rectangular ties. Cusson and Paultre [14] performed an experimental study to determine effects of variables such as the concrete compressive strength, the tie yield strength, the tie configuration, the transverse reinforcement ratio, the tie spacing, the longitudinal reinforcement ratio, and the spalling of the concrete cover. Then they proposed a stress strain model for confined high strength concrete [15]. Experimental behavior of steel fiber high strength concrete columns confined with low ratios

of rectangular ties under concentric compression is investigated by Junior and Giongo [16]. Braga and Laterza [17] and Assa et al [18] presented new approaches for confined concrete columns. As experimentally and analytically the magnitude of the strength enhancement of concrete confined was investigated by Chung et al [19]. Bousalem and Chikh[20] proposed an confined model for rectangular ordinary reinforced concrete columns in their study. An experimental study was made of confinement effectiveness of crossties in reinforced concrete columns subjected to monotonically increasing axial compression by Moehle and Cavanagh[21]. Abdel Halim and Abu Lebdeh [22] used finite element method to study the confinement of concrete by rectangular ties in reinforced-concrete tied columns. The strength and ductility of reinforced concrete beam and column cross-sections with varying geometries and levels of confinement were investigated using uncertainty analysis by Kappos et al [23]. An analytical model was proposed to construct a stress-strain relationship for confined concrete by Saatcioglu and Razvi [24]. Sharma et al carried out an experimental study to investigate the behavior of high strength short columns confined by circular spirals and square ties under monolithically increasing concentric compression. Test variables were volumetric ratio, spacing and yield strength of transverse reinforcement, longitudinal reinforcement ratio, transverse steel configuration, shape of cross section and compressive concrete strength in this study. Al-Shaikh [25] tested square tied concrete prisms under axial concentric compression. Tie spacing and diameter were defined as test variables in this study. Yong et al [5] reported the empirical results of a test program studying the effects of rectilinear confinement in high-strength concrete subjected to a monotonically increasing compressive axial load.

Although a lot of equations and approaches have been given for confined concretes with different concrete class and different reinforcement configurations in literature, it is not possible to use all parameters in a study and any general solution method hasn't been developed yet. Because of the requirement for much more extensive experimental studies, presenting a general approach or determination of general equations for all class reinforced concretes with different reinforcement properties and specimen properties etc., is really very difficult.

Recently, different ANN models have been applied in many engineering applications and proved to be very promising. Oreta and Kawashima [26] developed an ANN model with input parameters consisting of the unconfined compressive strength, core diameter, column height, yield strength of transverse reinforcement, volumetric ratio of transverse reinforcement, tie spacing, and longitudinal steel ratio to predict the confined compressive strength and corresponding strain of circular concrete columns. The ANN model proposed by Cevik and Guzelbey [27] is based on experimental results collected from literature to determine of strength enhancement of carbon fiber reinforced plastic confined concrete cylinders. Shear strength of circular reinforced concrete columns was determined by Caglar[28] using ANN techniques. Noorzaei et al[29], identified six input parameter that were cement, water, silica fume, super plasticizer, fine aggregate and coarse aggregate. Then, they developed an ANN model to predict compressive strength of concrete after 28 days. Tang et al [30], Mo et al [31], Lee [32], Yeh [33] and Guang and Zong [34], used ANN techniques for modeling confinement efficiency of reinforced concrete columns with rectilinear transverse steel for investigation of stress-strain relationship of confined concrete in hollow bridge columns, prediction of concrete strength, modeling of strength of high performance concrete and prediction of compressive strength of concrete respectively. There are much more investigations in literature about confined concrete and ANN. However, there hasn't been any performed study including normal and high strength concrete classes and transverse

reinforcement configurations to predict confined compressive strength of square concrete columns. In this study, an ANN model has been developed to find a general approach for confined square concrete columns.

2. An Overview of Neural Networks

ANNs are computer models of interactions between biological nerve cells (neurons) in human nervous system. Information processing unit called neuron is main component of an ANN model. There are four main parts in a biological neuron shown in Figure 1 [35]. The dendrites⁽¹⁾ are input path of a neuron. Signals from other neurons or environment are received by dendrites. The incoming signals from dendrites are summed in the cell body (soma)⁽²⁾. An impulse is produced and sent to the axon⁽³⁾ by the cell body if summed signals are greater than the threshold level of the neuron. Axon is output path of a neuron, splits up and connects to many dendrites through a junction called synapses⁽⁴⁾.

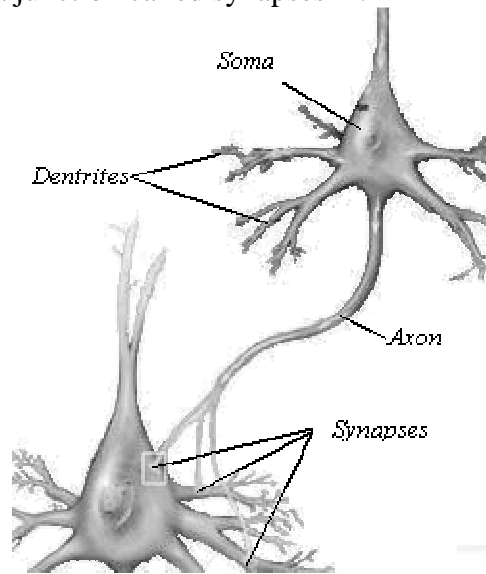


Figure 1. Main parts of a biological nerve cell [35]

Input wires, connection weights, activation functions and output wires take place instead of the dendrites, the synapses, the cell body (soma) and the axon respectively in ANNs. A mathematical neuron computes a weighted sum of its input signals with Equation 1 and generates an output by activation function. Many different mathematical functions are used as activation function in different ANN applications. Mostly, Threshold, Piecewise linear, Gaussian or Sigmoid function are preferred. Standard Sigmoid function defined by Equation 2 was used as activation function in this study. Generated outputs by neurons are either used as an input for next layer neurons or used results for output layer.

$$u_j = \sum_{i=1}^n w_{ij} x_i \quad (1)$$

$$f(u_j) = \frac{1}{1 + e^{-\beta(u_j - b_j)}} \quad (2)$$

Where, w_{ij} is the synaptic weight between neurons i and j , x_i is the input for neuron j , u_j , is the summation of n inputs for neuron j , b_j is the bias value of neuron j , $f(u_j)$ is the output of neuron j and β is slope parameter. Many different network topology (i.e. feedback, feed forward) and learning algorithm (i.e. supervised, unsupervised) have already been developed. In this present study multi layer feed forward neural network topology and back propagation

learning algorithm called generalized delta rule have been used. A feedforward artificial neural network and an artificial neuron are shown in Figure 2 (a) and in Figure 2 (b) respectively.

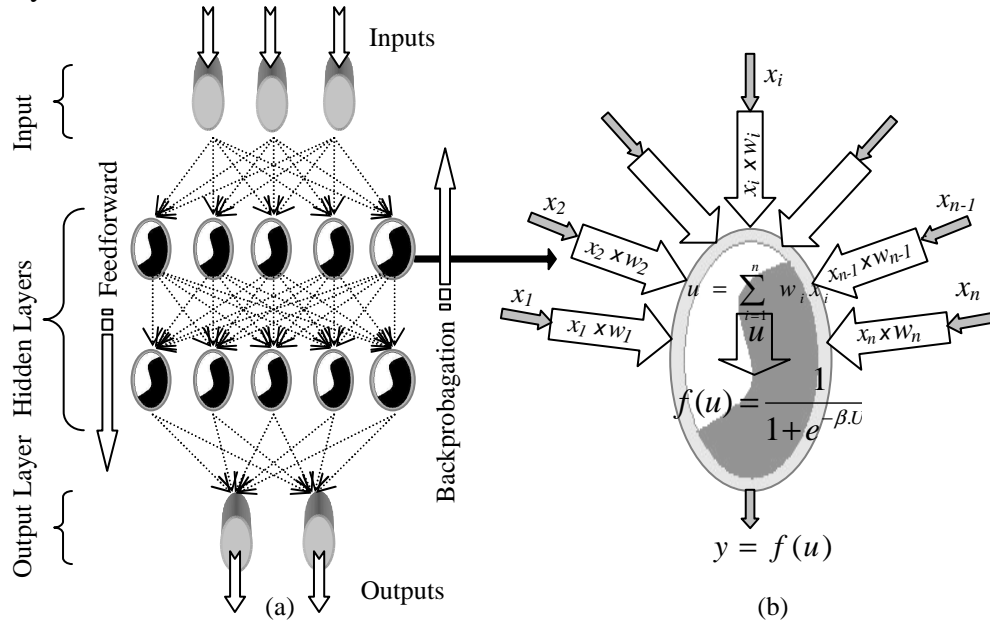


Figure 2. A feedforward artificial neural network^(a) and a neuron of artificial neural network^(b)

A multi layer feed forward neural network basically consist of an input layer, one or more hidden layer(s) and an output layer. Each layer has neuron(s). Numbers of neurons of input and output layers are the same with numbers of problem variables and problem outputs respectively. Determination of numbers of optimal layers and neurons in hidden layer is the most difficult tasks in multi layer feed forward neural network studies. This determination is generally made by trial and error approach based on type of problem, computational speed and computational accuracy. Synaptic weights and bias values of network allocated randomly at the beginning of training phase of multi layer feed forward neural network with back propagation learning algorithm. After network produce outputs, errors between the network outputs and desired outputs are calculated and propagate backward to the network. During back propagation of network error new synaptic weights are recalculated.

Trained neural network model has to be empirically validated using a selected test data that was not used in training. The validation of developed ANN model can be done with mean absolute error (MAE), mean squared error (MSE), root mean squared error (RMSE) and mean absolute percent error (MAPE) calculations. MAE, MSE, RMSE and MAPE definitions are given in 3rd, 4th, 5th and 6th equations respectively, where n , m , t and y are the number of test data, the number of output layer neurons, target value for the single neuron j and the output of a single neuron j respectively.

$$MAE = Mean \left(\sum_{i=1}^n \sum_{j=1}^m |t_{ij} - y_{ij}| \right) \quad (3)$$

$$MSE = Mean \left(\sum_{i=1}^n \sum_{j=1}^m (t_{ij} - y_{ij})^2 \right) \quad (4)$$

$$RMSE = \sqrt{Mean \left(\sum_{i=1}^n \sum_{j=1}^m (t_{ij} - y_{ij})^2 \right)} \quad (5)$$

$$MAPE = Mean \left(\sum_{i=1}^n \sum_{j=1}^m \frac{|t_{ij} - y_{ij}|}{y_{ij}} \right) \quad (6)$$

3. Confined Concrete Subjected Axial Compression

Confinement by transverse or lateral steel reinforcement improves the strength and ductility of reinforced concrete subjected axial compression. Uni-axial compression loading causes to laterally expanding and longitudinally contracting of confined concrete. Laterally expanding causes lateral pressure and lateral stresses in confined concrete. Transverse or lateral steel reinforcements resist against this lateral pressure. Resisting of transverse or lateral reinforcement increases axial load capacity of confined concrete.

Stress-strain relationships of confined or unconfined concrete subjected uni-axial loading describe their behavior. A lot of analytical models for stress-strain relationship of confined concrete were proposed in literature. Confined concrete strength is identified as maximum point of stresses in confined concrete models. Strength equations of some adopted confined concrete models are given in Table 1.

Table 1. Concrete strength equations of some adopted confined concrete models

Proposed by	Strength Equation(s)
Sheikh and Uzumeri[1]	$f_{cc} = 0.85 f_c' \left(1 + \frac{B^2}{140 \times 0.85 \times f_c' A_{cc}} \left(\left(1 - \frac{4C^2}{5.5B^2} \right) \left(1 - \frac{s}{2B} \right) \right) \sqrt{\rho_s f_s'} \right) \quad (3)$
Soliman and Yu[2]	$f_{cc} = 0.9 f_c' \left(1 + 0.05 \left(\left(1.4 \frac{A_{cc}}{A_c} - 0.45 \right) \frac{A_t (s_o - s)}{A_t s + 0.0028 s^2 B} \right) \right) \quad (4)$
Sargin[3]	$f_{cc} = \left(1 + 0.05468 \left(1 - 0.245 \frac{s}{b_e} \right) \frac{\rho_s f_y''}{\sqrt{f_c'}} \right) f_c' \quad (5)$
Nagashima [4]	$f_{cc} = 0.85 f_c' + 31.4 \sqrt{P_w' f_{yt} \left(1 - \frac{\sum C_i^2}{6B^2} \right) \left(1 - \frac{s}{2B} \right)^2} \quad (6)$
Yong et al. [5]	$f_{cc} = K f_c' = \left[1 + 0.11 \left(1 - \frac{0.245s}{h} \right) \left(\rho_s + \frac{nd''}{8sd} \rho \right) \frac{f_{yt}}{\sqrt{f_c'}} \right] f_c' \quad (7)$
Mugurama [6]	$f_{cc} = (1 + 49C_c) f_c' = \left(1 + 49 \left(0.313 \rho_s \frac{\sqrt{f_{yt}}}{f_c'} \left(1 - 0.5 \frac{s}{b} \right) \right) \right) f_c' \quad (8)$
Fafitis-Shah[7]	$f_{cc} = \left[1 + 15 \left(\frac{2A_{sh} f_{yt}}{sD_e f_c'} \right)^3 \right] \times \left[f_c' + \left(1.15 + \frac{21}{f_c'} \right) \times \frac{2A_{sh} f_{yt}}{sD_e} \right] \quad (9)$
Kappos [8]	$f_{cc} = 0.85 f_c' + 10.3 \left[\left(1 - \frac{\sum (b_i)^2}{6b_c d_c} \right) \left(1 - \frac{s}{2b_c} \right) \left(1 - \frac{s}{2d_c} \right) \rho_s f_{yh} \right]^{0.4} \quad (10)$
Mander [9]	$f_{cc}' = f_c' \left(-1.254 + 2.254 \sqrt{1 + \frac{7.94 f_l'}{f_c'} - 2 \frac{f_l'}{f_c'}} \right) \quad (11)$

4. Experimental Database

252 experimental data related to confined square concrete have been gathered from Chung et al.[35], Moehle and Cavannagh[21] , Razvi [37] , Sheikh and Uzumeri[38] , Cusson and Paultre[14, 15] , Junior and Giongo[16], Sugano et al.[39], Suzuki et al.[11], Hong et al.[10], Song et al.[12], Sharma et al.[24], Yong et al.[5], Nagashima et al.[4,37] and Li [37,41] by carrying out an extensive literature review. Because of some experimental data presented in the literature does not match the following criteria of this study, it could not be used in this study.

Geometric properties of confined concrete specimens and mechanical properties of concrete, transverse reinforcement and longitudinal reinforcement were taken as variables for this study. These variables are characteristic concrete strength obtained from compressive strength experiments, f_{ck} , side length of a square cross section, b , specimen highness, L , concrete cover, cc , yield strength of transverse reinforcement, f_{yt} , and longitudinal reinforcement, f_{yl} , diameter of transverse reinforcement, D_t , and longitudinal reinforcement, D_L , transverse reinforcement spacing, s , transverse reinforcement configuration types presented in Figure 3, $Type1(T_1)$, $Type2(T_2)$, $Type3(T_3)$, $Type4(T_4)$, $Type5(T_5)$ and $Type6(T_6)$, longitudinal reinforcement numbers at the corners, N_c , and at the sides, N_s , of the square cross section.

Longitudinal reinforcement diameter and number at the corners and at the sides in a cross section were used instead of longitudinal reinforcement ratio in order to take account into the geometrical effects of longitudinal reinforcement. Similarly, transverse reinforcement ratio had not been taken as a variable. Transverse reinforcement was represented by its diameter, its spacing and its configuration types in this study. The range of variables is listed in Table 2.

Table 2. Range of variables in experimental database

Parameters	Range
Characteristic concrete Strength, f_{ck} , (MPa)	20-128
Side length of a square cross section b , (mm)	150-305
Specimen highness, L , (mm)	381-1956
Concrete cover thickness, cc , (mm)	0-20
Spacing between two transverse reinforcement, s , (mm)	20-150
Yield strength of transverse reinforcement, f_{yt} , (MPa)	255-1387
Yield strength of longitudinal reinforcement, f_{yl} , (Mpa)	305,8-803
Diameter of transverse reinforcement, D_t	3,17-16
Diameter of longitudinal reinforcement, D_L	6-25
Longitudinal reinforcement number at the corners, N_c	0-4
Longitudinal reinforcement number at the sides, N_s	0-12
Transverse reinforcement types, $T_1, T_2, T_3, T_4, T_5, T_6$	0 or 1

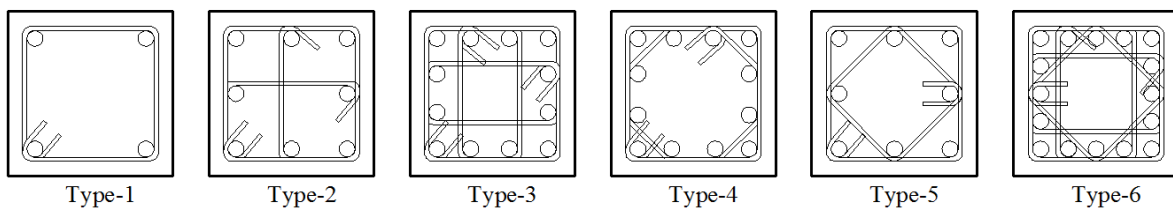


Figure 3. Transverse reinforcement configurations

Table 3 . Training sets for ANN (Continued)

No	Reference	Specimen	Inputs														Output			
			Concrete specimen				Transverse reinforcement						Long Reinforcement				Fcc (Mpa)			
			Fck (Mpa)	B (mm)	L (mm)	cc (mm)	Dt (mm)	Fyt (Mpa)	S (mm)	T1	T2	T3	T4	T5	T6	Nc		Dl (mm)	Fyl (Mpa)	Ns
136	Junior-Gio [16]	P1-24315	43	150	500	10,00	6,3	656	150	1	0	0	0	0	0	4	12,5	597	0	59,14
137		P1-268150	68	150	500	10,00	6,3	656	150	1	0	0	0	0	0	4	12,5	597	0	86,33
138		P1-26850	68	150	500	10,00	6,3	656	50	1	0	0	0	0	0	4	12,5	597	0	91,18
139		P1-291150	91	150	500	10,00	6,3	656	150	1	0	0	0	0	0	4	12,5	597	0	112,6
140		P1-29150	91	150	500	10,00	6,3	656	50	1	0	0	0	0	0	4	12,5	597	0	110,8
141	Al Shakhil [25]	C2	34	150	450	5,00	4	316	45	1	0	0	0	0	0	4	4	316	0	34,48
142		C3	33	150	450	5,00	4	316	60	1	0	0	0	0	0	4	4	316	0	33,66
143		C4	37	150	450	5,00	6	350	30	1	0	0	0	0	0	4	4	316	0	38,22
144		C7	43	150	450	5	8	380	30	1	0	0	0	0	0	4	4	316	0	41,87
145		C8	39	150	450	5,00	8	380	45	1	0	0	0	0	0	4	4	316	0	39,5
146	Suzuki et al. [11]	SF1P1Y3	46,3	250	750	0,00	6,4	1288	25	1	0	0	0	0	0	4	6	271	0	55
147		SF1P2Y1	46,3	250	750	0,00	6	317	50	1	0	0	0	0	0	4	6	271	0	48,83
148		SF1P2Y3	46,3	250	750	0,00	6,4	1288	50	1	0	0	0	0	0	4	6	271	0	49,79
149		SF1P3Y1	46,3	250	750	0,00	6	317	100	1	0	0	0	0	0	4	6	271	0	45,13
150		SF1P3Y2	46,3	250	750	0,00	6	1028	100	1	0	0	0	0	0	4	6	271	0	42,13
151		SF1P4Y3	46,3	250	750	0,00	6,4	1288	150	1	0	0	0	0	0	4	6	271	0	40,96
152		SF2P1Y3	84,8	250	750	0,00	6,4	1288	25	1	0	0	0	0	0	4	6	271	0	87,91
153		SF2P2Y1	84,8	250	750	0,00	6	317	50	1	0	0	0	0	0	4	6	271	0	80,52
154		SF2P2Y3	84,8	250	750	0,00	6,4	1288	50	1	0	0	0	0	0	4	6	271	0	79,15
155		SF2P3Y1	84,8	250	750	0,00	6	317	100	1	0	0	0	0	0	4	6	271	0	72,41
156		SF2P3Y2	84,8	250	750	0,00	6	1028	100	1	0	0	0	0	0	4	6	271	0	73,36
157		SF2P3Y3	84,8	250	750	0,00	6,4	1288	100	1	0	0	0	0	0	4	6	271	0	79,63
158		SF2P4Y3	84,8	250	750	0,00	6,4	1288	150	1	0	0	0	0	0	4	6	271	0	71,14
159		SF3P2Y1	128	250	750	0,00	6	317	50	1	0	0	0	0	0	4	6	271	0	114,9
160		SF3P2Y3	128	250	750	0,00	6,4	1288	50	1	0	0	0	0	0	4	6	271	0	111,05
161		SF3P3Y1	128	250	750	0,00	6	317	100	1	0	0	0	0	0	4	6	271	0	99,43
162		SF3P3Y2	128	250	750	0,00	6	1028	100	1	0	0	0	0	0	4	6	271	0	99,34
163	SF3P3Y3	128	250	750	0,00	6,4	1288	100	1	0	0	0	0	0	4	6	271	0	100,6	
164	SF3P4Y3	128	250	750	0,00	6,4	1288	150	1	0	0	0	0	0	4	6	271	0	111,27	
165	Song et al. [12]	1	24,3	150	600	4,50	9	306	70	1	0	0	0	0	0	4	9	305,8	0	34,85
166		2	24,3	200	800	6,50	12	306	95	1	0	0	0	0	0	4	12	305,8	0	35,28
167		3	24,3	200	800	3,00	6	306	32	1	0	0	0	0	0	4	6	305,8	0	33,25
168		4	24,3	200	800	4,50	9	306	70	1	0	0	0	0	0	4	9	305,8	0	33,57
169		5	24,3	200	800	6,50	12	306	130	1	0	0	0	0	0	4	12	305,8	0	33,2
170		6	24,3	200	800	4,50	9	306	38	1	0	0	0	0	0	4	9	305,8	0	34,05
171		7	24,3	200	800	6,50	12	306	70	1	0	0	0	0	0	4	12	305,8	0	38,68
172		8	24,3	200	800	0,80	16	306	123	1	0	0	0	0	0	4	16	305,8	0	31,43
173		9	24,3	180	540	4,50	9	306	60	1	0	0	0	0	0	4	9	305,8	0	36,12
174		10	24,3	180	720	4,50	9	306	60	1	0	0	0	0	0	4	9	305,8	0	34,15
175	Sharma et al. [24]	SA	62,2	150	600	10,00	8	412	50	1	0	0	0	0	0	4	12	395	0	68,34
176		SB	62,8	150	600	10,00	8	412	75	1	0	0	0	0	0	4	12	395	0	70,12
177		SC	61,85	150	600	10,00	8	520	50	1	0	0	0	0	0	4	12	395	0	67,04
178		SD	63,35	150	600	10,00	8	412	50	1	0	0	0	1	0	4	12	395	4	75,03
179		SPL	61,9	150	600	0,00	0	0	0	0	0	0	0	0	0	0	0	0	0	55,07
180		SE	82,5	150	600	10,00	8	412	30	1	0	0	0	0	0	4	12	395	0	86,57
181		SF	81,75	150	600	10,00	8	412	50	1	0	0	0	0	0	4	12	395	0	84,79
182		SG	83,15	150	600	10,00	8	412	75	1	0	0	0	0	0	4	12	395	0	91,78
183		SH	81,8	150	600	10,00	8	520	50	1	0	0	0	0	0	4	12	395	0	85,56
184	Yong et al. [5]	A	88,6	152	457	1,27	3,2	496	25,4	0	0	0	0	1	0	4	10	424	4	99
185		B	93,5	152	457	1,27	3,2	496	50,8	0	0	0	0	1	0	4	10	424	4	101,6
186		C	88,46	152	457	1,27	3,2	496	76,2	0	0	0	0	1	0	4	10	424	4	90,9
187		D	84,46	152	457	1,27	3,2	496	152	0	0	0	0	1	0	4	10	424	4	83,1
188		N	83,64	134	457	0,00	3,2	496	50,8	0	0	0	0	1	0	4	10	424	4	90,9
189		L	89,77	152	457	1,27	3,2	496	76,2	0	0	0	0	1	0	4	10	424	0	89
190	Nagashima et al. [4]	HH10LA	110	225	716	10,00	5,1	1387	45	0	0	1	0	0	0	4	10	378	8	122,5
191		HH13LA	110	225	716	10,00	5,1	1387	35	0	0	1	0	0	0	4	10	378	8	131,5
192		HH15LA	110	225	716	10,00	6,4	1368	45	0	0	1	0	0	0	4	10	378	8	127
193		HH20LA	112,1	225	716	10,00	6,4	1368	35	0	0	1	0	0	0	4	10	378	8	148,2
194		HL06LA	112,1	225	716	10,00	5	807	45	0	0	1	0	0	0	4	10	378	8	118,2
195		HL08LA	112,1	225	716	10,00	5	807	35	0	0	1	0	0	0	4	10	378	8	133,2
196		LL05LA	57,3	225	716	10,00	5	807	55	0	0	1	0	0	0	4	10	378	8	68,9
197		LL08LA	57,3	225	716	10,00	5	807	35	0	0	1	0	0	0	4	10	378	8	79,4
198		LH08LA	57,3	225	716	10,00	5,3	1387	55	0	0	1	0	0	0	4	10	378	8	70,9
199		LH13LA	57,3	225	716	10,00	5,1	1387	35	0	0	1	0	0	0	4	10	378	4	85,7

Table 3 . Training sets for ANN (Continued)

No	Reference	Specimen	Inputs															Output		
			Concrete specimen				Transverse reinforcement						Long. Reinforcement							
			Fck (Mpa)	B (mm)	L (mm)	cc (mm)	Dt (mm)	Fyt (Mpa)	S (mm)	T1	T2	T3	T4	T5	T6	Nc	Dl (mm)		Fyl (Mpa)	Ns
200	Nagashima et al.[4]	HH13MA	112,1	225	716	10,00	5,1	1387	35	0	0	1	0	0	0	4	8,16	596	8	131,8
201		HH13HA	112,1	225	716	10,00	5,1	1387	35	0	0	1	0	0	0	4	7,07	803	8	129,2
202		LL08MA	57,3	225	716	10,00	5	807	35	0	0	1	0	0	0	4	8,16	596	8	79,6
203		LL08HA	57,3	225	716	10,00	5	807	35	0	0	1	0	0	0	4	7,07	803	8	78
204		LH15LA	58,5	225	716	10,00	6,4	1368	45	0	0	1	0	0	0	4	10	378	8	88,7
205		HH13LB	112,1	225	716	10,00	5,1	1387	27	0	0	0	1	0	0	4	10	378	8	131,7
206		HH13LD	112,1	225	716	10,00	5,1	1387	25	0	0	0	0	1	0	4	10	378	4	128,2
207		LL08LD	58,5	225	716	10,00	5	807	25	0	0	0	0	1	0	4	10	378	4	77,3
208		HH13HSA	112,1	225	716	10,00	5,1	1387	35	0	0	1	0	0	0	4	7,07	803	8	134,8
209		LL08MSA	58,5	225	716	10,00	5	807	35	0	0	1	0	0	0	4	8,16	596	8	79
210		LL08HSA	58,5	225	716	10,00	5	807	35	0	0	1	0	0	0	4	7,07	803	8	80,05
211	Li [41]	1A	57	240	720	12,50	6	445	20	1	0	0	0	0	0	4	12,11	443	0	71
212		2A	57	240	720	12,50	6	445	20	0	0	0	0	1	0	4	12,11	443	4	90
213		4A	57	240	720	12,50	6	445	35	1	0	0	0	0	0	4	12,11	443	0	70
214		5A	57	240	720	12,50	6	445	35	0	0	0	0	1	0	4	12,11	443	4	71
215		7A	57	240	720	12,50	6	445	50	1	0	0	0	0	0	4	12,11	443	0	72,6
216		8A	57	240	720	12,50	6	445	50	0	0	0	0	1	0	4	12,11	443	4	72,6
217		10A	57	240	720	12,50	6	445	65	1	0	0	0	0	0	4	12,11	443	0	72
218		11A	57	240	720	12,50	6	445	65	0	0	0	0	1	0	4	12,11	443	4	72,4
219		1B	68,4	240	720	12,50	6	445	20	1	0	0	0	0	0	4	12,11	443	0	84,8
220		2B	68,4	240	720	12,50	6	445	20	0	0	0	0	1	0	4	12,11	443	4	107,4
221		4B	68,4	240	720	12,50	6	445	35	1	0	0	0	0	0	4	12,11	443	0	81,2
222		5B	68,4	240	720	12,50	6	445	35	0	0	0	0	1	0	4	12,11	443	4	81,5
223		7B	68,4	240	720	12,50	6	445	50	1	0	0	0	0	0	4	12,11	443	0	84,2
224		10B	68,4	240	720	12,50	6	445	65	1	0	0	0	0	0	4	12,11	443	0	73,1
225		11B	68,4	240	720	12,50	6	445	65	0	0	0	0	1	0	4	12,11	443	4	81,7
226		3HB1	49,4	240	720	12,50	6,4	1318	35	0	0	0	0	1	0	4	12,11	443	4	81,4
227		5HB	49,4	240	720	12,50	6,4	1318	50	0	0	0	0	1	0	4	12,11	443	4	61,6
228		3HC1	78,4	240	720	12,50	6,4	1318	35	0	0	0	0	1	0	4	12,11	443	4	105
229		5HC	78,4	240	720	12,50	6,4	1318	50	0	0	0	0	1	0	4	12,11	443	4	87,7
230	Bhow.[40]	CS17[31]	68,9	250	935	10,00	6,5	400	85	0	1	0	0	0	0	4	16	450	8	75,2
231	Suga. et al.[39]	200 NF	184	200	590	10,00	7,1	1400	35	0	0	1	0	0	0	4	10	685	8	235,8
232		160 NF	171	200	590	10,00	6	700	45	0	0	1	0	0	0	4	10	685	8	219,7

5. Determination of Optimum ANN architecture

Determination of optimum ANN architecture is the most difficult task in ANN studies. In order to design optimum ANN architecture, different ANN architectures were trained many times. Initial performances of the different ANN architectures were measured. All trainings were made for 1 percent error tolerance in a computer program coded using Visual Basic Program. Connection weights were selected randomly between 0 and 1 by computer program. Learning rate was 1, bias value was 0, training cycles was 25000 and number of training examples was 232 in all trainings made for initial performance evaluation.

MAE, MSE, RMSE and MAPE were used for the initial performance evaluation of different ANN architectures. Finally, 17-15-10-5-1 architecture was determined as the best ANN architecture. Selected ANN architecture with 17-15-10-5-1 configuration shown in Figure 4, refers to neuron numbers in input layer, first hidden layer, second hidden layer, third hidden layer and output layer respectively.

Table 4 . Testing sets for ANN

No	Reference	Specimen	Inputs															Output		
			Concrete specimen				Transverse reinforcement						Long Reinforcement							
			F _{ck} (Mpa)	B (mm)	L (mm)	cc (mm)	D _t (mm)	F _{yt} (Mpa)	S (mm)	T1	T2	T3	T4	T5	T6	N _c	D _L (mm)		F _{yl} (Mpa)	N _s
1	[10]	L8S7S3	20	200	600	17	6	700	30	1	0	0	0	0	0	4	12,7	420	4	26,86
2	[10]	M8S5.5S5.5	38,3	200	600	17	6	550	55	1	0	0	0	0	0	4	12,7	420	4	40,69
3	[10]	M8D5.5S4	40,2	200	600	17	6	550	40	0	0	0	0	1	0	4	12,7	420	4	64,92
4	[10]	H8S5.5S5.5	54	200	600	17	6	550	55	1	0	0	0	0	0	4	12,7	420	4	48,65
5	[37]	CS-8	124	250	1500	10	11,3	400	85	0	1	0	0	0	0	4	16	450	4	117,80
6	[37]	CS-17	81	250	1500	10	6,5	400	85	0	1	0	0	0	0	4	16	450	4	75,20
7	[37]	CS-26	60	250	1500	10	6,5	570	55	0	0	1	0	0	0	4	16	450	8	76,70
8	[38]	2C1-16	32,5	305	1956	19	3,17	589	50,8	0	0	0	0	0	1	4	13	407	12	37,60
9	[5]	1A	95,4	235	900	20	9,5	410	50	1	0	0	0	0	0	4	20	406	0	99,74
10	[2]	SF1P3Y3	46,3	250	750	0	6,4	1288	100	1	0	0	0	0	0	4	6	271	0	44,42
11	[2]	SF3P1Y3	128	250	750	0	6,4	1288	25	1	0	0	0	0	0	4	6	271	0	126,46
12	[16]	SI	82,55	150	600	10	8	412	50	0	0	0	0	1	0	4	12	395	4	86,45
13	[31]	HH08LA	110,04	225	716	10	5,1	1387	55	0	0	0	1	0	0	4	10	378	8	122,80
14	[41]	8B	68,4	240	720	12,5	6	445	50	0	0	0	0	1	0	4	12,11	443	4	80,50
15	[10]	M12S5.5E3	40,2	200	600	17	8	550	30	1	0	0	0	0	0	4	9,52	420	8	54,67
16	[10]	M12S5.5E5.5	39	200	600	17	8	550	55	1	0	0	0	0	0	4	9,52	420	8	43,43
17	[10]	H12S5.5E3	54	200	600	17	8	550	30	1	0	0	0	0	0	4	9,52	420	8	64,26
18	[10]	M12S9E5.5	39	200	600	17	8	900	55	1	0	0	0	0	0	4	9,525	420	8	44,75
19	[16]	CS-3	124	250	1500	10	6,5	570	55	0	0	1	0	0	0	4	16	450	8	129,1
20	[38]	2A1H-2	37	305	1956	19	4,76	255	57,1	0	0	0	0	1	0	4	16	367	4	39,6
21	[13]	10	27	200	400	10	10	404	200	0	0	0	0	1	0	4	13	376	4	28,5
22	[13]	15	26,3	200	400	10	10	404	75	0	0	0	0	1	0	4	13	376	4	42
23	[11]	SF1P3Y1	46,3	250	750	0	6	317	100	1	0	0	0	0	0	4	6	271	0	45,13
24	[24]	SPH	82,25	150	600	10	0	0	0	0	0	0	0	0	0	0	0	0	0	74,84
25	[41]	1HC1	78,4	240	720	12,5	6,4	1318	20	0	0	0	0	1	0	4	12,11	443	4	150

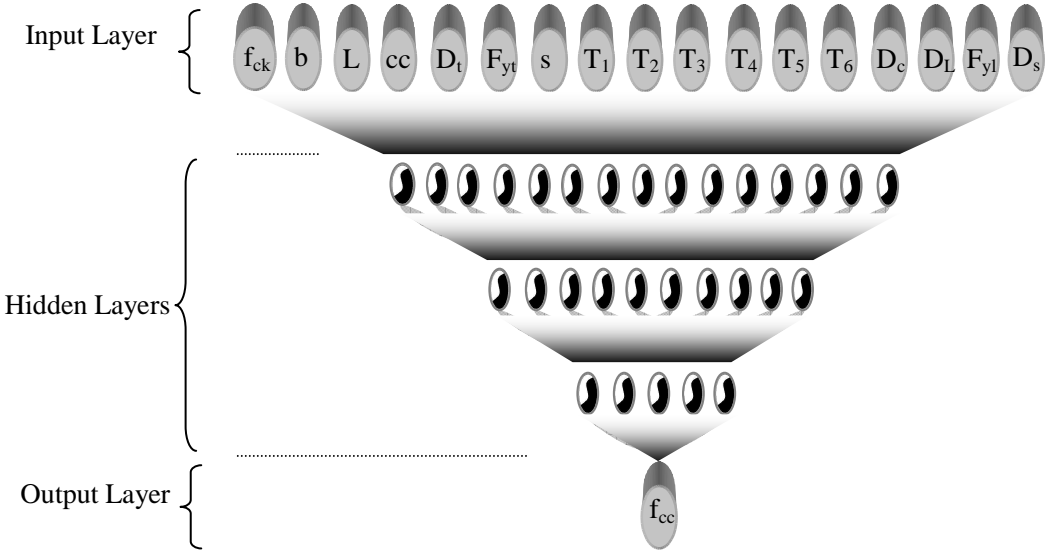


Figure 4. Determined artificial neural network architecture

6. Training and Testing of ANN Model

Among 252 data sets 25 confined square concrete data sets were selected randomly as testing sets. Remaining 232 data sets were used as training sets.

Training of the ANN model shown Figure 4 was completed at the 1.386.236th epoch with 0.099986 percent error and took about 5 ours, 41 minutes, and 55 seconds with a personal computer having 4 GB RAM and Intel Centrino 2 dual processors with 2.4 GHz for this network architecture. The error of network output was computed for each of the 1.386.236 epochs during training process and the network output error graphic shown in Figure 5 was obtained at the end of training process

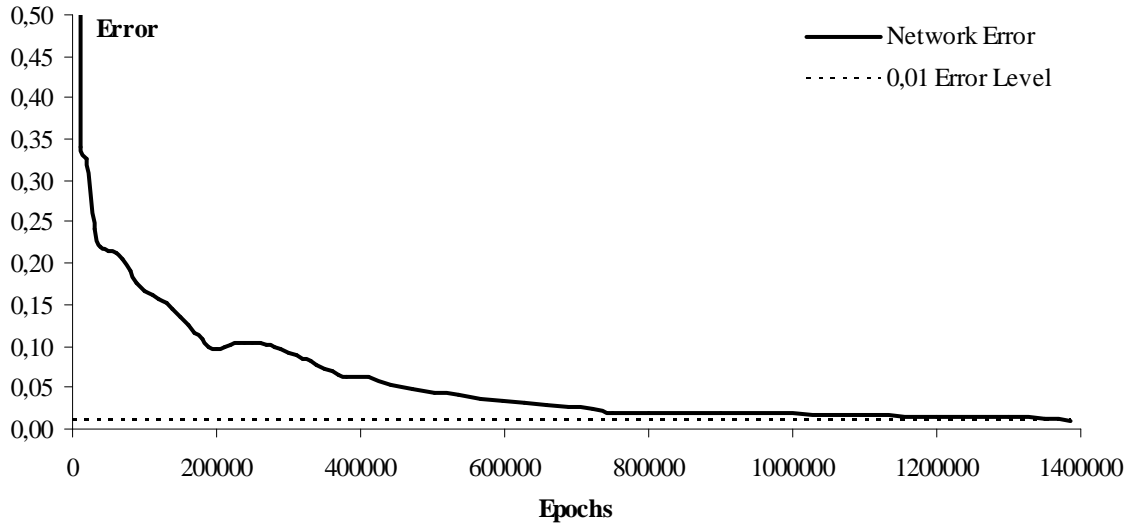


Figure 5. Calculated maximum output error for each epochs

After the training process, the ANN model was tested for experimental data given Table 4 by using final values of connection weights given in Table 5, Table 6, Table 7 and Table 8. ANN model validation based on the produced outputs by the ANN model for test data was done by final evaluation of network performance using MAE, MSE, RMSE and MAPE. The results of MAPE computations for each test examples were given in Table 9. Scaled target output values and network output with values between 0 and 1 were used in the MAE, MSE, RMSE and MAPE computations.

Predicted values by the ANN model, experimental results and % errors between of them were given for each test examples in Table 9. Minimum % error and maximum % error computed at the 5th and 20th test examples as 0,016 percent and 11,392 percent respectively. MAE, MSE, RMSE and MAPE values were obtained for test data as 0.00005030, 0.000295, 0.017162 and 0.04246944 respectively.

The correlation between predicted values by ANN model and actual values are given in Figure 6. The results of the ANN model are quite satisfactory. Correlation coefficient R^2 was computed as 0.9891.

7. Comparison of ANN Model with Analytical Models

Predicted confined concrete strength values by ANN model were compared with those of analytical models proposed by Sehih [1], Soliman Yu [2], Sargin [3], Nagashima [4], Yong et al. [5], Mugurama [6], Fafitis-Shah [7], Kappos[8] and Mander[9], using the same testing data. The comparison was done based on the ratio of $f_{cc}(model) / f_{cc}(experimental)$ and the statistical values which are MAE, MSE, RMSE, MAPE and R^2 . The ratio of $f_{cc}(model) / f_{cc}(experimental)$ for all analytical models and for ANN model is shown in Figure 7. As seen from this Figure, the predictions obtained by ANN model are generally closer to the experimental results than those of analytical models. Computed the statistical values were given in Table 10. It can be seen from Table 10 that, MAE, MSE, RMSE and MAPE values computed for ANN predictions are lesser than those of analytical models and the best correlation with experimental results was obtained by the developed ANN model. The further statistical details can be found in Table 10.

Table 5. Connection weights between input layer neurons and 1st hidden layer neurons

		INPUT LAYER NEURONS																
		1	2	3	4	5	6	7	8	9	10	11	12	13	14	15	16	17
1. HIDDEN LAYER NEURONS	1	3,404763	-0,46816	-2,35968	0,706821	3,814039	3,309432	7,29351	-1,89541	-2,46265	-0,78003	3,120209	-2,76932	2,375751	-3,4165	1,540422	1,55933	-1,94926
	2	5,533057	1,517056	0,691654	-4,00553	3,063648	-0,81514	0,147932	-0,63406	0,818611	0,850438	2,64435	1,90541	0,912343	-0,08239	2,579952	-5,19911	-6,64095
	3	-3,7419	-0,01466	-1,12594	1,091276	0,279086	3,418138	0,18264	-0,02363	-0,50365	0,716049	1,660942	-2,46062	1,544176	-1,26059	-0,18149	0,786772	-0,42682
	4	-1,33711	-0,90264	-1,0107	0,77236	2,424628	-1,39891	3,021724	-0,2631	1,062973	-1,11329	1,557368	-3,65576	1,237058	-0,46766	-0,14675	0,189708	0,569286
	5	4,905251	-2,24103	-1,42367	-2,30783	-0,06326	-3,6126	11,32983	0,147761	-1,02427	-2,56198	-1,57358	-1,32485	0,058974	-2,25504	-0,964	-0,77151	0,219398
	6	-5,03049	0,928427	-1,38216	-1,76134	-0,52495	-1,60822	0,340299	4,196373	-0,02756	-0,24959	1,443342	3,441586	0,909562	3,273165	1,66765	1,025557	-2,95038
	7	-1,96077	0,34321	-0,2183	-0,70271	-1,02756	-2,80101	2,156213	0,417032	0,968488	2,619358	1,074132	1,43618	0,474756	1,657331	1,646073	-3,93453	3,555992
	8	-7,81968	-6,8095	8,407908	-4,15645	-0,17195	2,074911	-10,7298	3,253836	1,030097	0,441178	-0,8335	2,405167	-2,33451	2,486483	0,963259	-1,22465	-1,53167
	9	3,639008	-1,79135	4,44202	0,47619	-8,33906	0,988867	21,10262	0,12787	-3,49537	-0,98161	1,529921	0,884938	1,068704	0,618421	-4,7474	4,782281	-3,54689
	10	11,20245	-2,3369	0,856401	-3,72242	1,635964	2,971514	-2,47787	1,84915	1,252445	-6,61064	3,293933	2,633947	4,199366	-0,8023	-3,56872	2,162139	-2,30827
	11	2,984905	-3,42621	-3,53565	-2,55021	5,396095	3,392438	8,007492	-0,04889	-2,07881	-4,70753	-2,20831	-1,0837	-1,45305	-1,68376	4,171904	-6,12844	-0,44473
	12	-2,14554	13,04979	1,832595	2,675974	1,491343	2,469266	-6,49327	-0,03966	-0,70217	-4,16646	0,142484	2,465377	-0,13407	-0,48662	-3,21186	-3,3589	-2,30134
	13	-5,78101	3,737784	-7,61338	-2,28898	-0,28127	0,6341	5,690173	-3,44659	-1,93576	4,702046	0,564832	-0,75599	0,05543	1,122407	4,333916	0,017079	-3,59351
	14	2,9832	2,560507	2,185542	-0,9594	-3,09183	-3,4489	1,952155	-2,01061	1,864199	-0,8567	-0,66458	0,107204	-0,86434	-1,81648	3,959429	-1,16901	0,225444
	15	2,957817	0,815117	0,112903	-2,34062	-0,82351	4,700035	6,590556	-0,5934	-0,98565	1,615169	2,341693	3,231116	2,832074	0,414061	-0,82729	0,799455	-2,8387

Table 6. Connection weights between 1st hidden layer neurons and 2nd hidden layer neurons

		1. HIDDEN LAYER NEURONS														
		1	2	3	4	5	6	7	8	9	10	11	12	13	14	15
2. HIDDEN LAYER NEURONS	1	-2,44584	1,687888	4,262293	2,451701	-3,0279	4,193442	-0,78862	-2,9685	4,803682	-3,91324	-0,98263	-3,25902	1,459408	3,031485	-1,37516
	2	-3,66527	-0,64241	1,646201	2,858426	0,996506	-0,47944	-0,06534	2,564867	-0,38758	-1,77679	0,792316	-1,64814	3,076381	1,336236	1,878935
	3	-0,32683	0,443659	0,155706	0,06248	0,449626	0,078654	0,140474	0,249314	0,535685	0,011326	0,045878	0,384298	0,946889	0,809904	0,967921
	4	-1,30039	-3,36838	1,317854	1,817215	-1,60566	2,656164	2,418554	1,940829	-0,88496	-0,85477	-3,27467	3,832158	-1,31379	0,118698	-0,2879
	5	-0,22245	1,253724	-1,36558	0,226058	2,344836	0,293579	-1,73848	1,010926	-0,42348	-1,08107	3,202812	-1,3179	1,125665	0,882341	1,248504
	6	0,440782	-4,08461	-0,97544	-1,41611	-0,29433	-2,13299	4,189603	2,006905	-2,40514	1,623173	3,559909	-2,52919	-0,72512	1,990602	-0,14905
	7	0,610258	-1,83189	-1,53051	1,758246	-5,84608	-4,20677	-0,96204	-7,18365	2,601094	0,95439	5,568372	2,681777	1,835857	0,178052	-0,85153
	8	-2,82526	1,619854	0,824357	-0,53581	-1,45631	-0,74918	-0,67834	4,012173	0,480323	1,011922	0,005692	-0,62223	2,198008	-0,65988	1,978686
	9	8,10888	6,925462	-0,22559	-1,96213	-4,654	0,948098	2,11999	-6,43645	-9,49992	4,723841	-6,86205	-6,91401	-10,0982	-3,59903	8,380149
	10	-1,29347	2,567315	0,633762	0,220574	2,719118	0,707364	-1,21123	3,176696	-1,39492	3,704457	-0,35144	-1,27575	-0,64041	1,91863	-5,18334

Table 7. Connection weights between 2nd hidden layer neurons and 3rd hidden layer neurons

		2. HIDDEN LAYER NEURONS									
		1	2	3	4	5	6	7	8	9	10
3. HIDDEN LAYER NEURONS	1	-4,2319286	-1,5739368	0,3699872	-0,5996829	-1,7708269	2,2297261	-6,2358576	-1,310003	7,1629557	0,5600051
	2	-2,3763474	0,9286609	2,2307929	4,6258242	2,3896913	4,0135551	-4,7361207	3,3403852	-6,5687285	-1,3247831
	3	-4,802948	4,869419	0,8999829	-0,4118514	-1,3879044	-5,298759	2,3561733	1,1301277	-12,243671	-3,5272771
	4	-4,0132029	-1,4921067	-0,426031	2,0915095	2,9343131	0,5282133	-0,6370812	-3,7477775	2,0929666	-0,7762604
	5	0,094513	-0,243952	-0,2553821	1,4389793	-1,1214142	0,6351964	-3,4272171	-1,7675155	-0,0026729	-2,74176

Table 8. Connection weights between 3rd hidden layer neurons and output layer neurons

		3. HIDDEN LAYER NEURONS				
		1	2	3	4	5
OUTPUT NEURON	1	6,070646	-0,67865	-6,44214	-1,83427	-2,35511

Table 9. % Error computations for each test examples

No	Speicemen	Exp. Results	ANN Outputs	Error (%)
1	L8S7S3 [10]	26,860	27,583	2,692
2	M8S5.5S5.5 [10]	40,690	38,209	6,096
3	M8D5.5S4 [10]	64,920	63,527	2,145
4	H8S5.5S5.5 [10]	48,650	51,278	5,402
5	CS-8 [37]	117,800	117,819	0,016
6	CS-17[37]	75,200	79,19	5,306
7	CS-26[37]	76,700	71,093	7,31
8	2C1-16[38]	37,600	39,737	5,682
9	1A[5]	99,740	89,556	10,21
10	SF1P3Y3[2]	44,420	44,596	0,397
11	SF3P1Y3[2]	126,460	126,512	0,041
12	SI[16]	86,450	88,141	1,955
13	HH08LA[31]	122,800	117,167	4,587
14	8B[41]	80,500	83,127	3,264
15	M12S5.5E3[10]	54,670	53,435	2,259
16	M12S5.5E5.5[10]	43,430	45,251	4,192
17	H12S5.5E3[10]	64,260	59,073	8,072
18	M12S9E5.5[10]	44,750	56,111	0,287
19	CS-3[16]	129,100	134,304	4,031
20	2A1H-2[38]	39,600	35,089	11,392
21	10[13]	28,500	28,538	0,135
22	15[13]	42,000	38,064	9,372
23	SF1P3Y1[11]	45,130	49,857	10,475
24	SPH[24]	74,840	74,881	0,055
25	1HC1[41]	150,000	151,198	0,799
Mean Error (%)				4,247
Standart Deviation				3,613

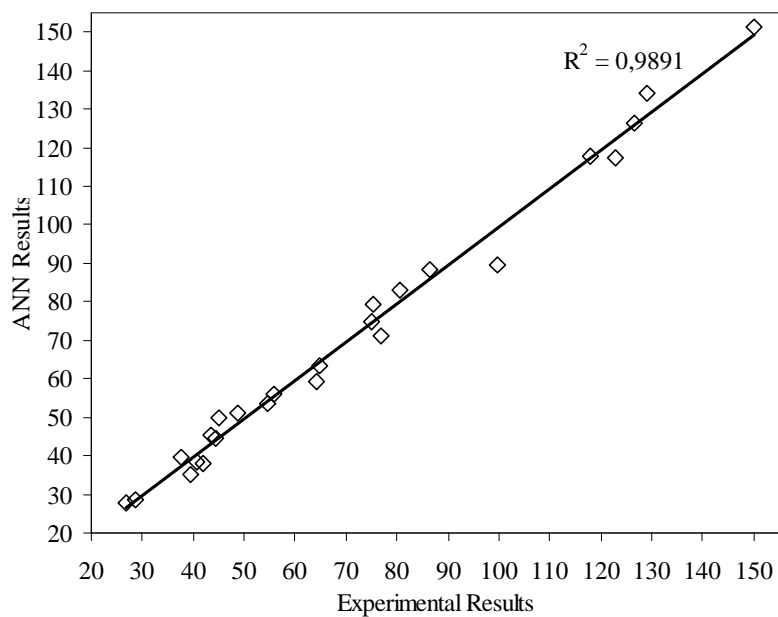


Figure 6. The correlation between predicted values by ANN model and experimental results

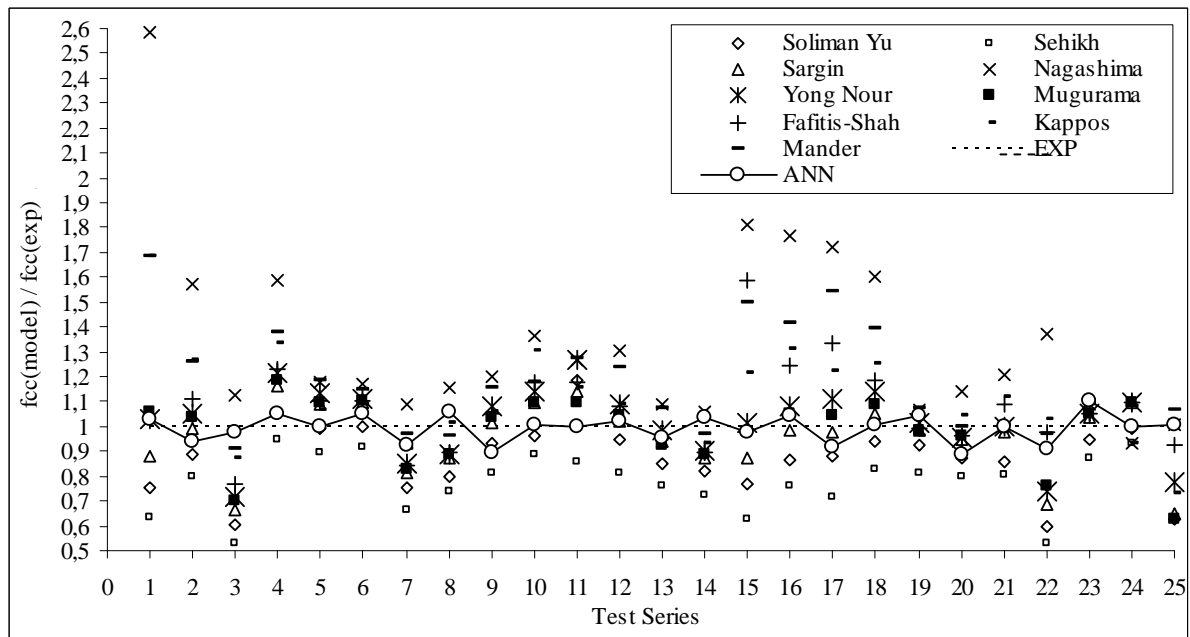


Figure 7. Ratios of proposed model results and ANN outputs to experimental results

Table 10. MAE, MSE, RMSE, MAPE and R^2 values for the results of analytical models and ANN predictions

	MAE	MSE	RMSE	MAPE	R^2
Sehikh [1]	0,000267	0,008447	0,091906	0,236065	0,804256
Soliman Yu[2]	0,00017	0,003965	0,062965	0,146919	0,852963
Sargin[3]	0,000138	0,003016	0,054923	0,107821	0,859133
Nagashima[4]	0,000305	0,007969	0,089272	0,344076	0,837801
Yong et al. [5]	0,000144	0,002572	0,050715	0,112185	0,889916
Mugurama[6]	0,000135	0,003041	0,055145	0,101865	0,851791
Fafitis-Shah[7]	0,000188	0,002446	0,049459	0,222603	0,815556
Kappos[8]	0,000166	0,002709	0,052048	0,161953	0,876158
Mander[9]	0,000208	0,004346	0,065924	0,199099	0,919232
ANN	5,03E-05	0,000295	0,017166	0,042469	0,989102

8. Summary and Conclusion

An ANN application for prediction of confined compressive strength of square concrete columns was presented in this study. In addition to the 11 physical and mechanical properties of confined concrete specimens, 6 different confinement configurations were defined as input variables. The optimum ANN architecture was obtained by many trials. The results obtained from the developed ANN model were compared with those of analytical models and experimental studies. The developed ANN model predicted closer outputs to the experimental results than the analytical models with less errors. This conclusion shows that developed neural network model can be used in compressive strength predictions of confined normal and high strength ($f_{ck} = 20\sim 184$ MPa) square concrete columns for the 6 different confinement configurations defined in this study.

The % errors (MAPE) of 9th, 21th and 23th testing sets were obtained 10.210 %, 11.392 %, and 10.475 % respectively. The errors of remaining 22 testing sets were computed below 10 %. Mean % error obtained 4.247 with 3.613 standard deviation. Different experimental conditions and other parameters were not defined as variables in this study. Hence, these error results can be seen acceptable.

Some variables, like hook angle, hook type, elasticity modulus of materials, Poisson ratio of materials, new longitudinal and transverse reinforcement configurations, etc. were not used in this study because of the lack of experimental data. This study can be developed by using these and any other variables for confined concrete columns.

9. References

- [1]. Sheikh, S. A., and Uzumeri, S. M., Analytical Model for Concrete Confinement in Tied Columns Journal of the Structural Division, 108 (1982) 2703-2722.
- [2]. Soliman MTM and Yu, C.W., The Flexural Stress–Strain Relationship of Concrete Confined by Rectangular Transverse Reinforcement. Mag. Concr. Res., 19 (1967) 223–238.
- [3]. Sargin M. Stress–Strain Relationships for Concrete and the Analysis of Structural Concrete Sections. Solid Mechanics Division, Study No: 4, University of Waterloo, 1971.
- [4]. Nagashima, T., Sugano S., Kimura H. and Ichikawa, A., Monotonic Axial Compression Test on Ultra-High-Strength Concrete tied Columns, Proc. of 10th World Conf. on Earthquake Engineering, 5 (1992) 2983-2988.
- [5]. Yong, Y.K., Nour, M.G. and Nawy, E.G., Behavior of Laterally Confined High-Strength Concrete Under Axial Loads, Journal of Structural Engineering, (1988) 332-351
- [6]. Mugurama H, Watanabe F, Iwashimizu T, Mitsueda R Ductility improvement of high-strength concrete by lateral confinement. Trans. of Japan Concrete Institute, 5 (1983) 403–410.
- [7]. Fafitis A, Shah S P, Predictions Of Ultimate Behavior Of Confined Columns Subjected To Large Deformations J. Am. Concret. Inst., 82 (1985) 423–433.
- [8]. Kappos A.J., Chryssanthopoulos, M.K., Dymmiotis C., Uncertainty Analysis of Strength and Ductility of Confined Reinforced Concrete Members, Engineering Structures, 21 (1999) 95–208.
- [9]. Mander, J.B., Priestley, M.J.N. and Park, R., Theoretical Stress Strain Model for Confined Concrete, ASCE Structural Journal, 114 (1988) 1804-1826.
- [10]. Hong, K.N., Han, S.H. and Yi, S.T., High-Strength Concrete Columns Confined By Low-Volumetric-Ratio Lateral Ties, Engineering Structures, 28 (2006) 1346–1353.
- [11]. Suzuki, M., Akiyama, M., Hong, K.N., Cameron, I.D. and Wang, W.L., Stress-Strain Model Of High-Strength Concrete Confined By Rectangular Ties, 13th World Conference on Earthquake Engineering, Paper No: 3330, Vancouver, B.C. Canada, August 2004.
- [12]. Song, H.W., Choi, D.H., Byun, K.J. and Maekawa, K., Analyses of Concrete Columns Confined with Lateral Reinforcements, Annual Conference of JCI, 20 (1998) 91-96.
- [13]. K. Sakai, S. A. Sheikh, Y. Kakuta and T. Ohta: Confinement by Rectilinear Ties in Reinforced Concrete Columns, Proceedings of Pacific Concrete Conference, Auckland, New Zealand, 1988.
- [14]. Cusson D. and Paultre, P., High-Strength Concrete Columns Confined by Rectangular Ties, Journal of Structural Engineering, 120 (1994) 783-804.

- [15]. Cusson D. and Paultre, P., Stress-Strain Model for Confined High Strength Concrete, *Journal of Structural Engineering*, 121 (1995) 468-477.
- [16]. Junior, H.C.L, Giongo, J.S., Steel-Fibre High-Strength Concrete Prisms Confined by Rectangular Ties Under Concentric Compression, *Materials and Structures*, 37 (2004) 689-697.
- [17]. Braga F, Laterza, M., A New Approach to the Confinement of R/C Columns 11th European Conference On Earthquake Engineering, Balkema, Rotterdam, 1998.
- [18]. Assa B., Nishiyama, M. and Watanabe F., New Approach for Modeling Confined Concrete, *Journal of Structural Engineering*, 127 (2001) 751-757.
- [19]. Chung, H.S., Yang, K.H, Lee, Y.H, and Eun, H.C, Strength and Ductility of Laterally Confined Concrete Columns, *Can. J. Civ. Eng.*, 29 (2002) 820–830.
- [20]. Bousselam, B. and Chikh, N., Development of a Confined Model for Rectangular Ordinary Reinforced Concrete Columns, *Materials and Structures*, 40 (2006) 605–613.
- [21]. Moehle, J.P., ASCE, A.M., and Cavannagh, T., Confinement Effectiveness of Crossties in RC, *Journal of Structural Engineering*, 111 (1985) 2105-2120.
- [22]. Abdel-Halim M.A.H., and Abu-Lebdeh, T.M., Analytical Study For Concrete Confinement in Tied Columns, *Journal of Structural Engineering*, 115 (1989) 2810-2828.
- [23]. Saatcioglu, M., Razvi, S. R., Strength and Ductility of Confined Concrete, *Journal of Structural Engineering*, 118 (1992) 1590-1607.
- [24]. Sharma, U.K., Bhargava, P. and Kauskik, S.K., *Journal of Advanced Concrete Technology*, 3 (2005) 267-281.
- [25]. Al Shaikh, A., Stress-Strain Relationship for Concrete confined by Rectilinear Reinforcement: A Stiffness Degradation Approach, *J.King Saud Univ. Eng. Sci(2)*, 6 (1993) 149-166.
- [26]. Oreta A.W.C. and Kawashima K., Neural Network Modeling of Confined Compressive Strength and Strain of Circular Concrete Columns, *Journal of Structural Engineering*, 129, (2003) 554-561.
- [27]. Cevik, A. And, Güzelbey I.H, Neural Network Modeling Of Strength Enhancement for Cfrp Confined Concrete Cylinders, *Building and Environment*, 43 (2008) 751–763.
- [28]. Caglar, N., Neural Network Based Approach for Determining the Shear Strength of Circular Reinforced Concrete Columns, *Construction and Building Materials*, 23 (2009) 3225–3232.
- [29]. Noorzaei, J., Hakim, S.J.S. , Jaafar, M.S., and Thanoon W.A.M., Development of Artificial Neural Networks for Predicting Concrete Compressive Strength, *International Journal of Engineering and Technology*, 4 (2007) 141-153.
- [30]. Tang, C.W., Chen, H.J., and Yen, T., Modeling Confinement Efficiency of Reinforced Concrete Columns with Rectilinear Transverse Steel Using Artificial Neural Networks, *J. Structural. Engineering*. 29 (2003) 775-783.
- [31]. Mo Y.L., Hung H.Y. and Zhong J., Investigation of Stress-Strain Relationship of Confined Concrete in Hollow Bridge Columns Using Neural Networks, *Journal of Testing and Evaluation*, 330-339.
- [32]. Lee, S.C., Prediction of Concrete Strength Using Artificial Neural Networks, *Engineering Structures*, 25 (2003) 849-857.
- [33]. Yeh, C., Modeling of Strength of High Performance Concrete Using Artificial Neural Networks, *Cement and Concrete Research*, 28 (1998) 1797-1808.
- [34]. Ni Hong-Guang, N., Ji-Zong W., Prediction of compressive strength of concrete by neural Networks, *Cement and Concrete Research*, 30 (2000) 1245-1250.
- [35]. <http://www.memorydr.com/images/alz13.jpg>, 01.02.2010.

- [36]. Chung, H.S., Yang, K.Y., Lee, Y.H. and Eun, H.C., Stress–Strain Curve of Laterally Confined Concrete, *Engineering Structures*, 24 (2002) 1153–1163.
- [37]. Razvi S., Confinement of Normal and High Strength Concrete Columns, Philosophy Thesis, University of Ottawa, Ottawa, Canada, June 1995.
- [38]. Sheikh, S.A., and Uzumeri, S.M., “Strength and Ductility of Tied Concrete Columns, *Journal of Structural Engineering, ASCE*, 106 (1980) 1079-1102.
- [39]. Sugano, S., Kimura, H., Shirai, K., Study of New RC Structures Using Ultra-High-Strength Fiber-Reinforced Concrete(UFC)-The Challenge of Applying 200 MPa UFC to Earth-quake Resistant Building Structures, *Journal of Advanced Concrete Technology*, 5 (2007) 133-147.
- [40]. Bhowmick R., Sharma U., and Bhargava P., Numerical Simulation of Confined Concrete Columns and a Parametric Study, *Asian Journal Of Civil Engineering (Building And Housing)*, 7 (2006) 269-286.
- [41]. Li B., Strength and Ductility of Reinforced Concrete Members and Frames Constructed Using High Strength Concrete, Research Report No. 94-5 University of Canterbury, Christchurch, New Zealand, p.389, May 1994.